Investigation of Through Thickness Residual stress Distribution in Equal Channel Angular Rolled Al 5083 Alloy by Layer Removal Technique and X-ray Diffraction

M. Mahmoodi [a], M. Sedighi [a*], D.A. Tanner [b]

[a] School of Mechanical Engineering, Iran University of Science and Technology, Tehran, Iran

[b] Materials and Surface Science Institute (MSSI), University of Limerick, Limerick , Ireland

[*] Correspondence: sedighi@iust.ac.ir Tel +98-21-77491228 Fax +98-21-77240488

Abstract

The layer removal technique and the x-ray diffraction method have been employed to evaluate the residual stresses through the thickness of aluminium alloy 5083 processed by equal channel angular rolling (ECAR). ECAR is a severe plastic deformation process that introduces shear deformation to sheet metals. The process has been completed on 2 mm thick strips passed three times through die channels in a continuous manner. In this work, the profile of residual stresses was quantitatively determined. It was observed that after ECAR process, the residual stress magnitudes were changed from approximately zero in annealed condition up to half of the yield strength value of ECARed samples. The distribution of the residual stresses was found to be non-uniform through the thickness and the ECARed sample was compressive at the top surface while it was tensile at the bottom surface.

Keywords: Non-ferros metals and alloys (A), X-ray analysis (G), Elastic behaviour (F).

1. Introduction

Residual stresses are self equilibrium internal stresses that exist in manufactured parts with no external forces and constraints [1]. Equal channel angular rolling (ECAR) is a severe plastic deformation method where the material can experience large strain magnitudes [2]. In this process, the material is passed through the channel of dies without changing the cross-sectional area of the strip [3]. Therefore it can be utilized in different passes to obtain ultrafine grain and desirable material properties [4,5].

In metal forming processes where material undergoes plastic deformation, different plastic strain deformation at the same times in different locations creates an internal stress distribution. One reason for different actual strains is due to the shape of deformation zone that exerts a strong effect on the magnitude and distribution of residual stresses.

For a material with a specific yield point, residual stresses as a pre-stress state causes a change in the yield strength [6]. In addition, the residual tensile stresses on the material surface are undesirable as it can lead to reduced fatigue life and make the material vulnerable to stress corrosion cracking [7–9]. The methods of non-destructive, destructive and semi destructive measurement can be applied to measure the residual stresses. In destructive methods such as layer removal method, the strain variation caused in relieving the residual stresses in the material is measured. For applying this method it is important to have information about the nature of the residual stresses field that is, magnitude and distribution of stresses in one, two or three directions [1].

Considering the layer removal technique there are some assumptions for the stress field in sheets, strips, wires and plates. The stress distribution can be assumed biaxial in the plane of

the sample and vary through the thickness [10,11] or it can be uniform [12]. The layer removal technique and x-ray diffraction are applicable procedures to measure the biaxial residual stresses over the planar surface of the sheet or metal strips. The stresses on the plane of sample are assumed constant. Also this technique has been applied to determine the residual stress in thin films and coatings [13,14].

The residual stresses distribution has been studied for cold and hot forming processes such as extrusion, wire drawing and rolling, but the magnitude and the distribution of residual stresses in the strips and sheet metals processed by ECAR, has not been evaluated up to now. The sheet metals are widely used in the transportation industries and it is important to know the specifications of the sheet metal such as residual stress distribution. In some of sheet products, the amount of residual stress is not considerable and a few works have been done for residual stress measurement in sheet metals produced by a forming process. Therefore the study of residual stress in ECARed materials is became a necessity. In this article, the methods of layer removal and x-ray diffraction have been utilized to determine the residual stress through the thickness in material processed by equal channel angular rolling.

2. Experimental Procedure

2.1. Material

In this research, a 2 mm thick sheet of aluminium alloy 5083 was used. At first, the material was cut to samples with the dimensions of 400 mm×40 mm×2 mm (length×width×thickness). Then they were annealed at 450˚C for 1 hour before ECAR which minimized the residual stresses in the samples. The residual stress of near zero was measured after annealing. The chemical composition (in wt %) of the material is listed in Table 1.

Table1: Chemical composition (in wt.%) of Al 5083 alloy

2.2. Equal channel angular rolling process

A schematic of the ECAR machine used to introduce the shear deformation into metal strip is illustrated in figure 1-a. It was equipped by two feeding rolls and dies.

Fig. 1: a- A schematic showing the equal channel angular rolling process b- Channel angles in forming zone

The thickness of the inlet and outlet channel is 2 mm. In figure 1-b, the oblique angle (Φ) which is the intersection angle of outlet and inlet channels is 130° and the curvature angle (Ψ) is 0°. The Al strip having the initial thickness of 2 mm is fed through the feeding rolls and reduced into the 1.95 mm thick strip. After passing from the forming zone, the sample retains its initial thickness (2 mm). In the present work, the feed speed is 3 m/min and the Al strip is ECARed in three passes. The route A has been selected to do the process. In route A, the sample is fed through the channel with no rotation between the passes around the x direction. It is assumed that the top and bottom surfaces of the sample are respectively in contact with the upper and lower dies.

Using Eq. (1) the effective strain imposed to the material per 3 passes is 1.54.

$$\varepsilon_{eff} = \frac{2N}{\sqrt{3}} . K^2 \cot\left(\frac{\Phi}{2}\right) \quad (1)$$

In Eq. (1), N is the number of passes, Φ the oblique angle and K=0.975 is the thickness ratio. This formula is obtained from the modified Segal model for calculation of shear deformation [2]. It is assumed that the dimensional change of length, width and thickness of the metal strip is negligible. The Al 5083 sample processed by ECAR at room temperature has been represented in figure 2.

Fig. 2: Al 5083 sample processed by ECAR after 3 passes through route A with a small curvature

2.3. Residual stress measurement by layer removal technique and XRD

In this research, the layer removal technique and x-ray diffraction method have been carried out to determine the residual stresses through the sample thickness. Electropolishing was applied for removing the material as a thin layer. It creates a flat surface and removes the material without affecting material below. For this procedure, sample and solution (electrolyte) form the part of DC electrical circuit. The Lacomit varnish was used for masking the sample to prepare only the area to be polished in contact with the electrolyte. The electropolishing was carried out using Barker's reagent (5 ml Fluoroboric acid in 200 ml water) at room temperature and the optimum voltage and current were 30 V and 1 A.

In order to do the layer removal, the layer thickness removed in each increment of electropolishing test was 0.2 mm. The thickness in each increment was controlled with a micrometer.

Before using the layer removal technique, the x-ray diffraction method was applied to determine the residual stress magnitudes at the surface. The stresses have been measured in each increment in longitudinal(x) and transverse (y) directions. Figure 3 shows the schematic of stress measurement by x-ray diffraction method.

Fig. 3: A schematic of x-ray diffraction for stress measurement

The PANalytical's X'Pert PRO MRD system has been applied to do the experimental measurement. Cu Kα radiation with $\lambda = 1.54056$ Å was used as x-ray source in the irradiated area of 5 mm which λ is the x-ray wavelength. The diffraction angle, 2θ ranges from 134° to

138°. For each measurement, 14 steps were employed and the exposure time for each step was 20 s to ensure the appropriate intensity. The generator tension (voltage) and current were 40 kV and 40 mA. The residual stress analysis has been done by the $\sin^2\psi$ technique. The angular positions of the diffraction peak were selected for positive ψ tilts of equal intervals from 0 to 50°.

3. Results and discussion

In order to investigate the residual stresses through the thickness, a biaxial plane stress state has been assumed and the two-angle $\sin^2\psi$ technique has been performed (The stress component σ_{33} in z direction of the strip surface is zero). After correction for Lorentz polarization and absorption effects, the Pearson VII function was used to indicate the position, breadth and the diffracted intensity of the $K\alpha_1$ diffraction peak.

Figure 4 shows the calculated residual stress σ_{11} along the longitudinal direction at the top surface of the ECARed sample before the material removal in d-$\sin^2\psi$ plot [15]. It should be noted that the sample before the ECAR process was annealed and the residual stresses measured by XRD was approximately zero.

Fig. 4: d(hkl) versus $\sin^2\psi$ plot for an Al 5083 sample processed by ECAR after 3 passes

Then, using electropolishing the material was removed for subsurface measurement. The stresses were measured in rolling direction after each layer removal at different depths from the top surface of sample.

As stressed layers of material are removed, the remaining stresses in the sample and on the exposed surface are changed [16]. Therefore, it is necessary that the subsurface residual stress measurement be corrected for the removal of prior surface layers.

For correcting the measured stresses and calculating the true residual stresses, it is assumed that the residual stresses in the flat sample depend on the distance from the top surface, except near the edges. The corrected (true) stresses $\sigma_x(z_1)$ at depth z_1 have been represented by Eq. (2) [1].

$$\sigma_x(z_1) = \sigma_{x_m}(z_1) + 2\int_{z_1}^{H} \frac{\sigma_{x_m}(z)}{z} dz - 6z_1 \int_{z_1}^{H} \frac{\sigma_{x_m}(z)}{z^2}\, dz \tag{2}$$

Where $\sigma_{x_m}(z_1)$ is the measured stress at depth z_1, H is the original thickness of the sample and z_1 is the distance from the bottom surface to uncovered depth of interest (new thickness after material removal). Figure 5 shows the biaxial plane stress during layer removal.

Fig. 5: Biaxial plane stress in Al 5083 sample during layer removal

Eq. (3) expresses the correction in stress $C(z_1)$ as the difference between the measured stress and true stress at z_1 [1].

$$C(z_1) = 2\int_{z_1}^{H} \frac{\sigma_{x_m}(z)}{z} dz - 6z_1 \int_{z_1}^{H} \frac{\sigma_{x_m}(z)}{z^2}\, dz \tag{3}$$

In this work, the H=2 mm and the removed layer in each stage is 0.2 mm. Employing the Eqs. (2) and (3) the true residual stress along the roll direction σ_{11} and the correction in the stresses were calculated.

Figure 6 shows the profile of residual stress through the thickness along the longitudinal direction or roll direction. According to this figure, the profile of residual stress is not uniform and changes from the tensile condition to compressive. The residual stress on the top

surface is compressive, but on the bottom surface is tensile. The maximum residual tensile stress is 123 MPa at the depth of 0.8 mm and the maximum compressive residual stress is -165 MPa at the depth of 1 mm.

In figure 6 considering the obtained results of residual stresses in last 5 increments, the probability bounds for this method of calculation get wider by increasing the depth.

Fig. 6: Profile of residual stress σ_{11} through the thickness in the Al 5083 sample processed by ECAR

The residual stress values σ_{22} in transverse (width) direction were determined after each layer removal at different depths from the top surface of sample. Using Eqs. (2) and (3), the true residual stress σ_{22} and the correction in the stresses were calculated.

Figure 7, shows the profile of residual stress through the thickness perpendicular to the roll direction. According to this figure, the profile of residual stress is not uniform and changes from the tensile condition to compressive. The maximum residual tensile stress is 59 MPa and the maximum compressive residual stress is -93 MPa.

Fig. 7: Profile of residual stress σ_{22} through the thickness in the Al 5083 sample processed by ECAR

It should be pointed out that when the residual stresses are removed from the material by layer removal technique, the internal stresses and moments have to be in balance. In this work applying the results of residual stresses, Eq. (4) shows the forces and bending moments associated with residual stresses are initially balanced in the ECARed sample.

$$\int \sigma(z)dz \simeq 0 \tag{4}$$

Where $\sigma(z)$ can be the residual stresses σ_{11} and σ_{22} at depth z [17].

Figure 8, shows the residual stresses σ_{11} and σ_{22} in comparison to each other. The profile of residual stresses σ_{11} through the thickness is similar to σ_{22}, but the magnitude of residual stresses σ_{11} is greater than σ_{22}.

Fig. 8: Comparison of residual stresses profiles σ_{11} and σ_{22} in the Al 5083 sample processed by ECAR

According to these results, the process of equal channel angular rolling introduce the non-uniform residual stress to the non stress annealed sample as the top surface is completely different with bottom surface. It can be assumed that when the metal strip passes through the deformation zone, the bending and then straightening deformation take place on the material. Therefore large stress gradient exists through the material thickness before passing the sample from the die set. The region from the neutral axis to the top surface of sample is entirely tensile while it is compressive to the bottom surface. After passing the sample from the die set, the springback effect changes the stress distribution and causes the non uniform distribution of residual stresses.

As it is shown in figure 2, this difference can only be observed as the curvature due to the spring back effect in the ECARed sample which is upward. Tang [18] showed that for predicting the springback in anisotropic aluminium alloys, consideration of the Bauschinger effect is essential.

On the other hand, the surface quality of a product is determined by residual stress distribution since its presence can shorten the service life of the component when used under severe service conditions. Unlike the SPD process such as shot peening and deep rolling that only introduce compressive residual stress at the surface [19-21], ECAR causes the different

surface residual stress as the stress at the bottom surface is tensile. Therefore this distribution has to be considered in applying the ECARed sheet in service condition or latter process.

It can be said that, equal channel angular rolling introduces remarkable residual stresses to the sheet metal in comparison with other sheet metal forming such as rolling [22]. The processes of rolling, deep rolling and shot peening cannot introduce non-uniform residual stresses to the sheet the same as the ECAR process.

Combining the layer removal technique with rapid XRD in comparison with measuring the sample curvature is a simple and cost effective approach as well a good alternative for accurate evaluating the stress profiles in sheet metals such as ECARed samples [1,6,23].

Figure 9 shows the effects of ECAR Process on the yield strength and the flow stress of Al 5083 sample. The mechanical properties were determined utilizing ASTM E8, Standard Test Methods for Tension Testing of Metallic Materials [24]. A clear yield phenomenon and a reduction in the tensile ductility could be observed for the ECARed specimen compared with the annealed specimen. According to this figure the yield strength of the annealed sample is 165 MPa, but it has been increased up to 300 MPa after 3 passes ECAR which is almost twice larger than that for the annealed ones. In addition, the effective strain imposed to the ECARed material is 1.54. This magnitude of strain could be obtained in rolling with nearly 75% reduction in thickness. Although, the residual stresses distribution (shown in figure 8) could potentially has an influence on yielding criterion, but its mechanism will be complicated and needs independent investigation.

Fig. 9: The stress-strain curves for the annealed sample and ECARed one of Al 5083 alloy

4. Conclusion

The layer removal technique and x-ray diffraction method were applied to determine the through thickness residual stresses distribution in Al sample processed by ECAR. It was shown that the presented method can be effective in determination of the residual stress profile for ECARed strip and sheet metals.

According to the results, the ECAR process introduced the non-uniform residual stress in both direction x and y to the non stress annealed sample with the maximum of compressive stress at the depth of 1 mm and tensile stress at the depth of 0.8 mm. It was expressed that the sample was compressive at the top surface and was in tension at the bottom surface in both direction x and y. The profile of residual stresses σ_{22} along the transverse direction y was similar to the profile of residual stress along the longitudinal direction x, but at less magnitude.

It was also observed that the ECAR process changed the level of yielding strength almost twice larger than the annealed ones. Further investigation is suggested for studying the effect of residual stress field on yielding criterion of ECARed samples.

Acknowledgments

This work has been carried out as a part of sabbatical in the Materials and Surface Science Institute (MSSI), University of Limerick in Ireland; additionally, our gratitude goes to Dr Jeremy Robinson, for his help on undertaking the layer removal technique by electropolishing process.

References

[1] Totten G, Howes M, Inoue T. Handbook of residual stress and deformation of steel. ASM International 2002; Materials Park, Ohio

[2] Lee J Ch, Seok H K, Han J H, Chung Y H. Controlling the textures of the metal strips via

the continuous confined strip shearing(C2S2) process. Materials Research Bulletin 2001; 36:997–1004

[3] Nakashima K, Horita Z, Nemoto M, Langdon T G. Development of a multi-pass facility for equal-channel angular pressing to high total strains. Materials Science and Engineering A 2000; 281: 82-87

[4] Iwahashi Y, Horita Z, Nemoto M, Langdon T G. The process of grain refinement in equal-channel angular pressing. Acta Materialia 1998; 46:3317–3331

[5] Nam C Y, Han J H, Chung Y H, Shin M C, Effect of precipitates on microstructural evolution of 7050 Al alloy sheet during equal channel angular rolling. Materials Science and Engineering A 2003; 347:253–257

[6] Ekmekçi B, Ekmekçi N, Tekkaya A E, Erden A. Residual stress measurement with layer removal method. First Cappadocia International Mechanical Engineering Symposium 2004; Turkey

[7] Yang F, Jiang J Q, Fang F, Wang Y, Ma C. Rapid determination of residual stress profiles in ferrite phase of cold-drawn wire by XRD and layer removal technique. Materials Science and Engineering A 2008; 486:455–460

[8] Ghosh S, Rana V P, Kain V , Mittal V , Baveja S K. Role of residual stresses induced by industrial fabrication on stress corrosion cracking susceptibility of austenitic stainless steel. Materials and Design 2011; 32:3823–3831

[9] Constantinescu A, Oueslati A. On the reconstruction of residual stresses after matter removal in rods. C R Mecanique 2008; 336:69–78

[10] Treuting R G , Read W T. mechanical determination of biaxial residual stress in sheet materials. Journal of Applied Physics. 1951; 22:2:130–134

[11] Read W T. Formulas for the Determination of Residual Stress in Wires by the Layer Removal Method. Journal of Applied Physics 1951; 22:4:415-416

[12] Gunnert R. Residual Welding Stresses, Method of Measuring Residual Stresses and Its Application to a Study of Residual Welding Stresses. Alquist E. Wicksell 1955; Stockholm

[13] Massl S, Köstenbauer H, Keckes J, Pippan R. Stress measurement in thin films with the ion beam layer removal method: Influence of experimental errors and parameters. Journal of Thin Solid Films 2008; 516:8655–8662

[14] Lima C R C, Nin J, Guilemany J M. Evaluation of residual stresses of thermal barrier coatings with HVOF thermally sprayed bond coats using the Modified Layer Removal Method (MLRM). Journal of Surface & Coatings Technology 2006; 200: 5963–5972

[15] Prevéy P S. X-ray Diffraction Residual Stress Techniques. Metals Handbook, Metals Park, American Society for Metals1986; 10:380-392

[16] Hornbach D J, Prevéy P S, Mason P W. X-ray diffraction characterization of the residual stress and hardness distributions in induction hardened gears. Proceedings First International Conference on Induction Hardened Gears and Critical Components, Gear Research Institute 1995; 69-76

[17] Sglavo V M, Bonafini M, Prezzi A. Procedure for residual stress profile determination by curvature measurements. Mechanics of Materials 2005; 37: 887–898

[18] Tang B, Lu X, Wang Z, Zhao Z. Springback investigation of anisotropic aluminum alloy sheet with a mixed hardening rule and Barlat yield criteria in sheet metal forming. Materials and Design 2010; 31:2043–2050

[19] Kim T, Lee J H, Lee H, Cheong S k. An area-average approach to peening residual stress under multi-impacts using a three-dimensional symmetry-cell finite element model with plastic shots. Materials & Design 2010; 31:1: 50–59

[20] Franchim A S, Campos V S, Travessa D N, Moura Neto C. Analytical modeling for residual stresses produced by shot peening. Materials & Design 2009; 30:5:1556–1560

[21] Juijerm P, Altenberger I. Effective boundary of deep-rolling treatment and its correlation

with residual stress stability of Al–Mg–Mn and Al–Mg–Si–Cu alloys. Scripta Materialia 2007;56:745–748

[22] Razny W, Fischer F D, Finstermann G, Schwenzfeier W, Zeman K. The influence of some rolling parameters on the residual stresses after rolling. Proceedings of the 6th International Conference on Metal Forming 15 June 1996; 60: 1–4: 81–86

[23] Bendek E, Lira I, Francois M, Vial C. Uncertainty of residual stresses measurement by layer removal. Journal of Mechanical Sciences 2006; 48:1429–1438

[24] ASTM E 8-04, Standard Test Methods for Tension Testing of Metallic Materials, Annual Book of ASTM Standards, Vol 03.01, American Society for Testing and Materials, Philadelphia; 2005

Table caption:

Table1: Chemical composition (in wt.%) of Al 5083 alloy

Figure caption:

Fig. 1: a- A schematic showing the equal channel angular rolling process b- Channel angles in forming zone

Fig. 2: Al 5083 sample processed by ECAR after 3 passes through route A with a small curvature

Fig. 3: A schematic of x-ray diffraction for stress measurement

Fig. 4: d(hkl) versus $\sin^2\psi$ plot for an Al 5083 sample processed by ECAR after 3 passes

Fig. 5: Biaxial plane stress in Al 5083 sample during layer removal

Fig. 6: Profile of residual stress σ11 through the thickness in the Al 5083 sample processed by ECAR

Fig. 7: Profile of residual stress σ22 through the thickness in the Al 5083 sample processed by ECAR

Fig. 8: Comparison of residual stresses profiles σ11 and σ22 in the Al 5083 sample processed by ECAR

Fig. 9: The stress-strain curves for the annealed sample and ECARed one of Al 5083 alloy

Figures and Tables

Table1: Chemical composition (in wt.%) of Al 5083 alloy

Al	balance
Mg	4.5
Mn	0.75
Cr	0.15
Fe	max 0.1
Si	max 0.1

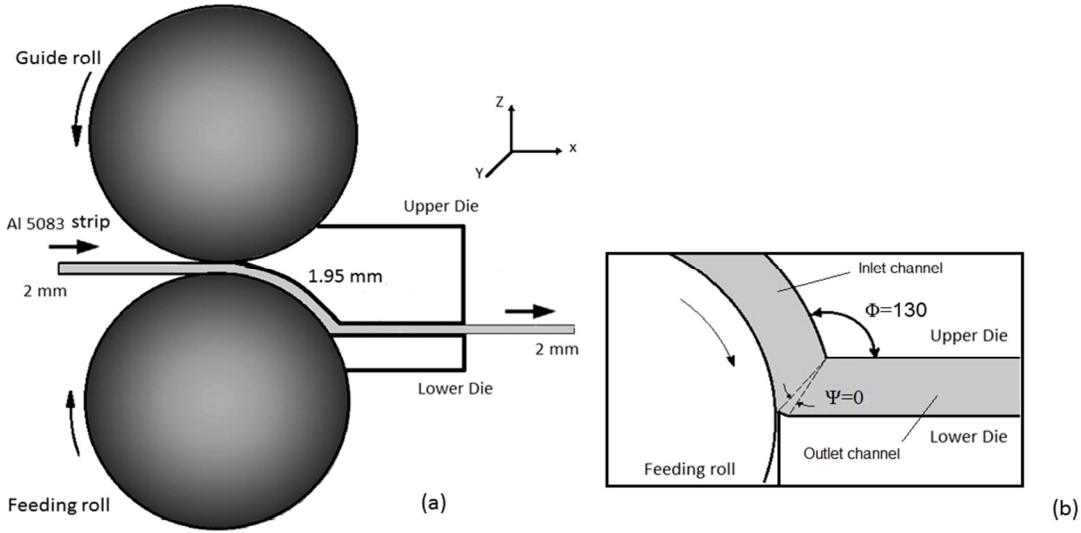

Fig. 1: a- A schematic showing the equal channel angular rolling process b- Channel angles in forming zone

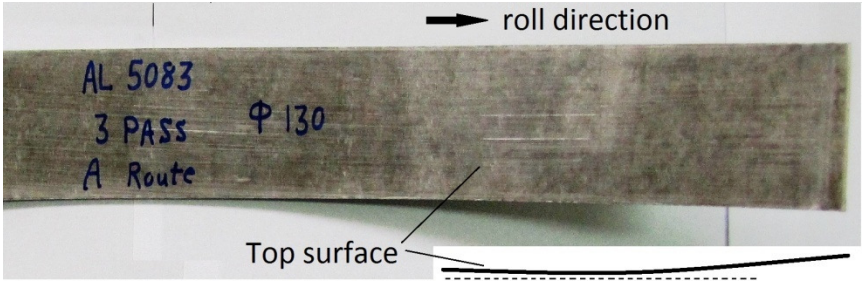

Fig. 2: Al 5083 sample processed by ECAR after 3 passes through route A with a small curvature

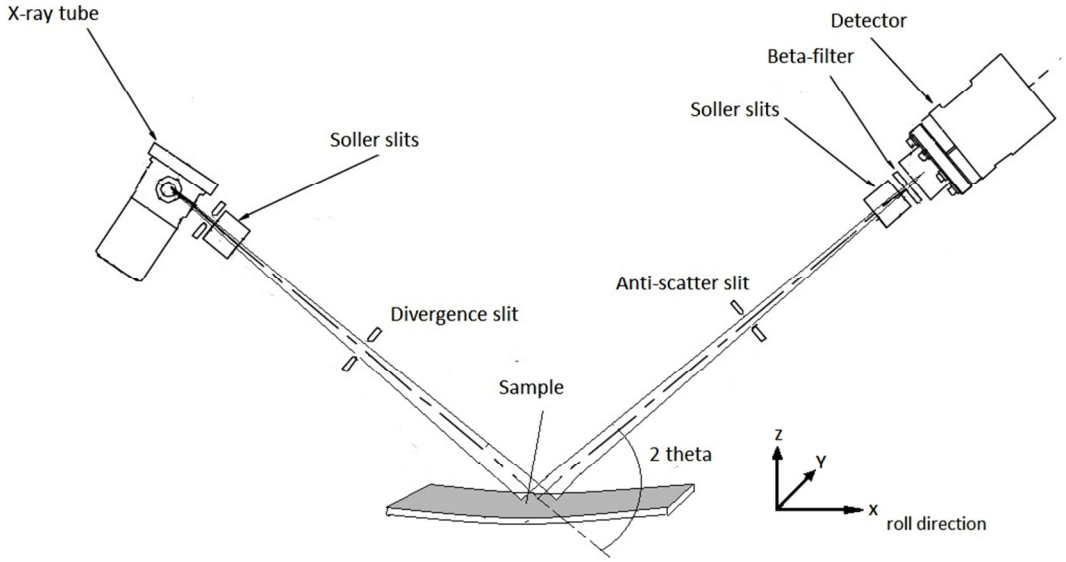

Fig. 3: A schematic of x-ray diffraction for stress measurement

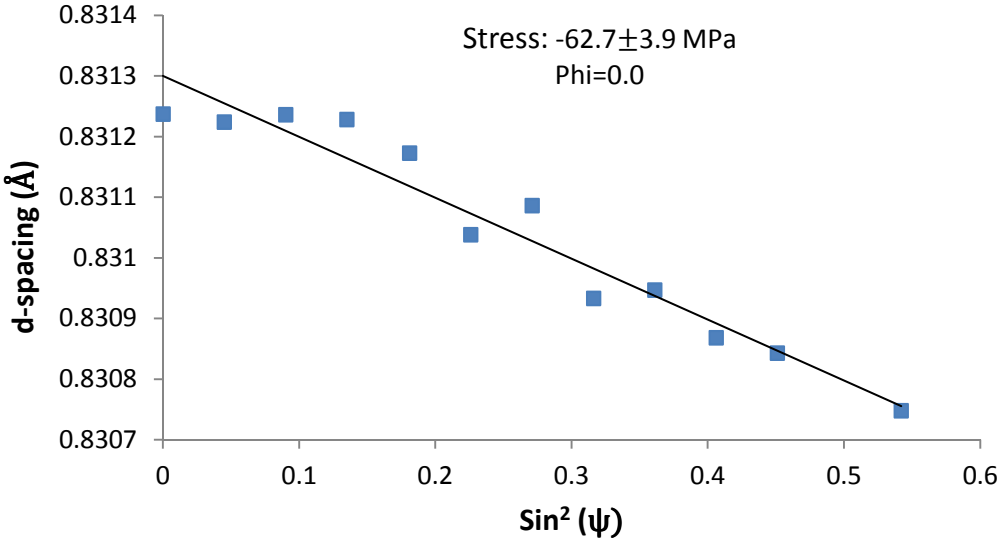

Fig. 4: d(hkl) versus $sin^2\psi$ plot for an Al 5083 sample processed by ECAR after 3 passes

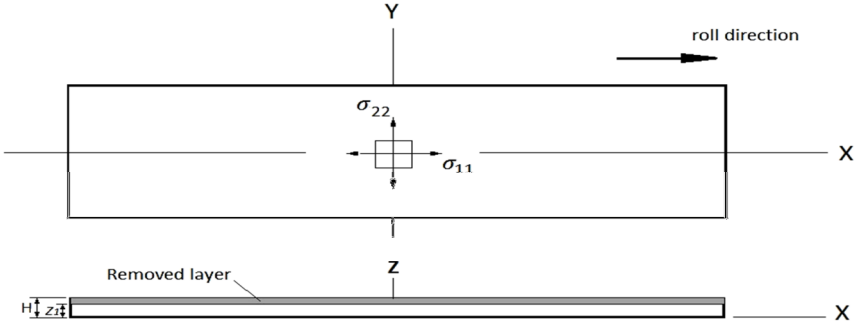

Fig. 5: Biaxial plane stress in Al 5083 sample during layer removal

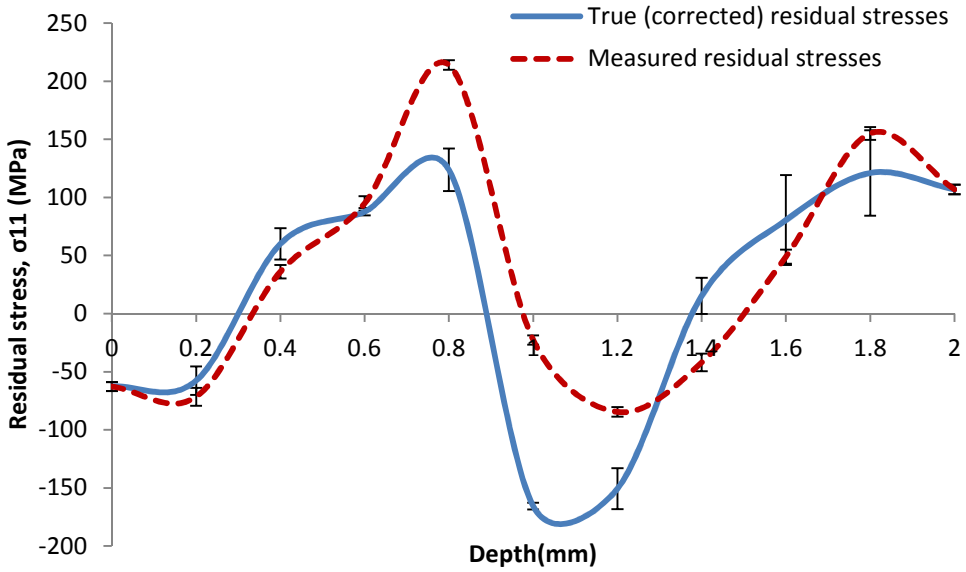

Fig. 6: Profile of residual stress σ_{11} through the thickness in the Al 5083 sample processed by ECAR

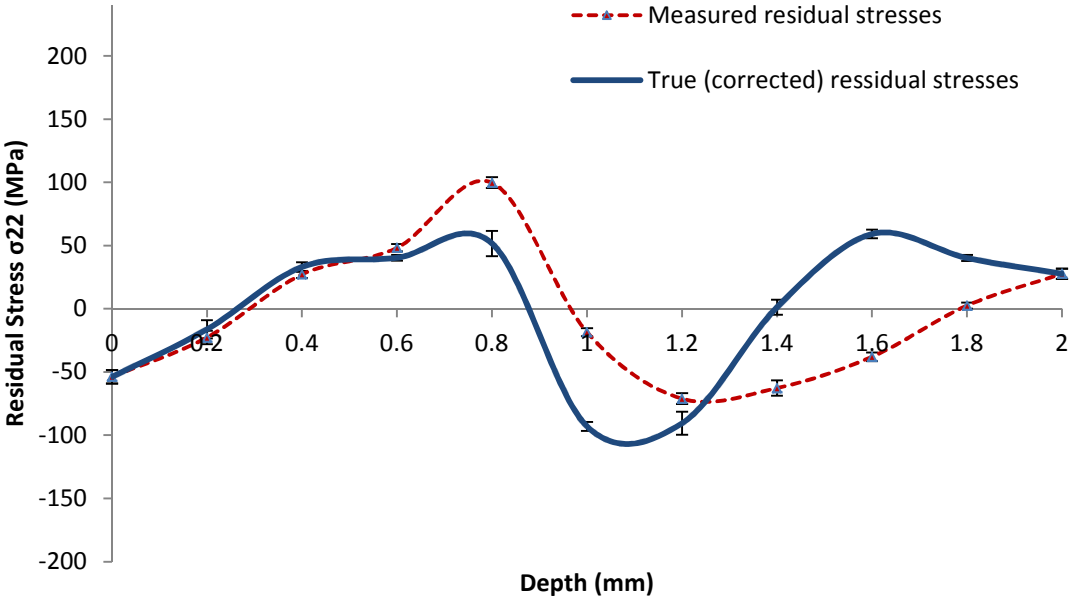

Fig. 7: Profile of residual stress σ_{22} through the thickness in the Al 5083 sample processed by ECAR

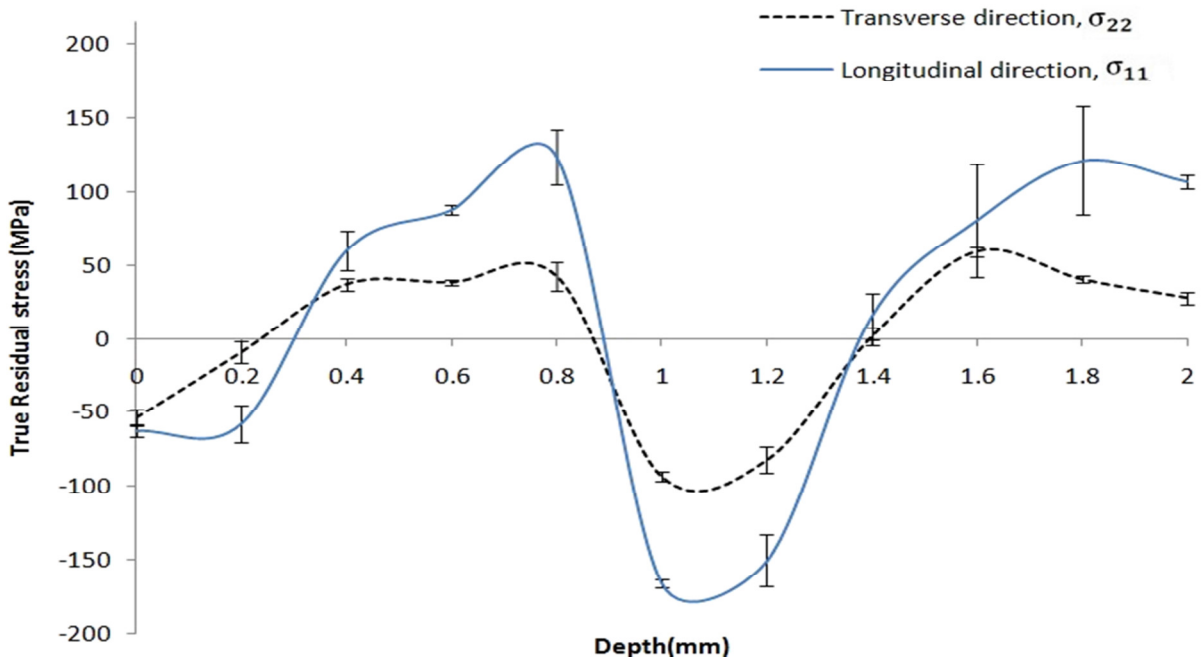

Fig. 8: Comparison of residual stresses profiles σ_{11} and σ_{22} in the Al 5083 sample processed by ECAR

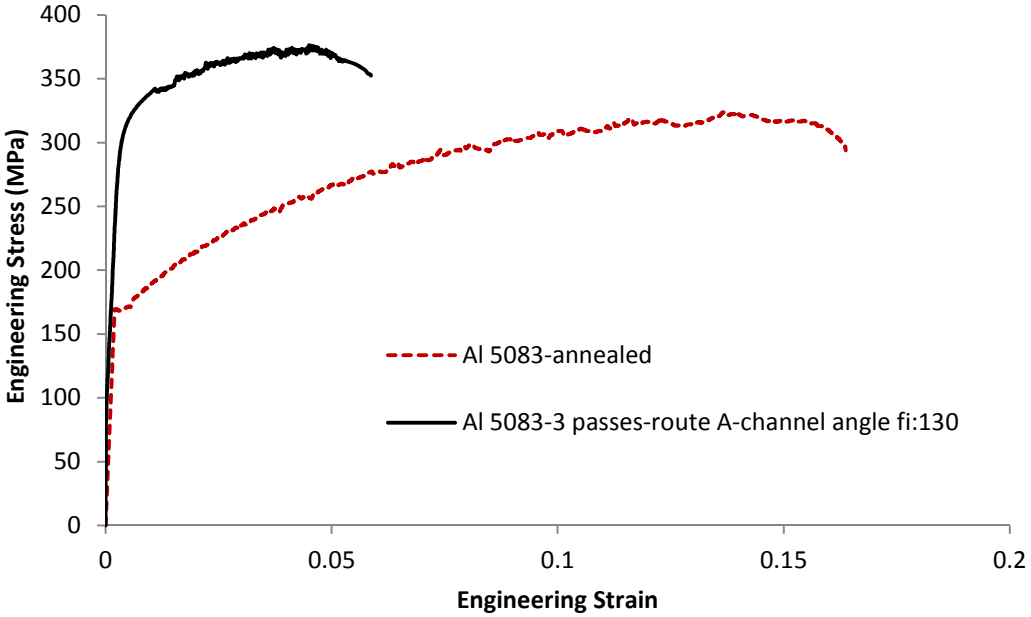

Fig. 9: The stress-strain curves for the annealed sample and ECARed one of Al 5083 alloy